Searching for GUT-scale QCD axions and monopoles with a high-voltage capacitor

Michael E. Tobar,[1,*] Anton V. Sokolov,[2] Andreas Ringwald,[3] and Maxim Goryachev[1]
[1]*Quantum Technologies and Dark Matter Labs, Department of Physics, University of Western Australia, 35 Stirling Highway, Crawley, Western Australia 6009, Australia*
[2]*Department of Mathematical Sciences, University of Liverpool, Liverpool, L69 7ZL, United Kingdom*
[3]*Deutsches Elektronen-Synchrotron DESY, Notkestraße 85, 22607 Hamburg, Germany*

(Received 20 June 2023; accepted 2 August 2023; published 17 August 2023)

The QCD axion has been postulated to exist because it solves the strong-*CP* problem. Furthermore, if it exists axions should be created in the early Universe and could account for all the observed dark matter. In particular, axion masses of order 10^{-10} eV to 10^{-7} eV correspond to axions in the vicinity of the grand unified theory scale (GUT-scale). In this mass range many experiments have been proposed to search for the axion through the standard QED coupling parameter $g_{a\gamma\gamma}$. Recently axion electrodynamics has been expanded to include two more coupling parameters, g_{aEM} and g_{aMM}, which could arise if heavy magnetic monopoles exist. In this work we show that both g_{aMM} and g_{aEM} may be searched for using a high-voltage capacitor. Since the experiment is not sensitive to $g_{a\gamma\gamma}$, it gives a new way to search for effects of heavy monopoles if the GUT-scale axion is shown to exist, or to simultaneously search for both the axion and the monopole at the same time.

DOI: 10.1103/PhysRevD.108.035024

I. INTRODUCTION

The axion is a putative pseudo-Goldstone boson of Peccei-Quinn (PQ) symmetry breaking, thought to exist because it solves the strong-*CP* problem [1–7]. Furthermore, the axion is a prime candidate for cold dark matter because it is predicted to be created in the early Universe and can account for all of the observed cold dark matter [8–11]. One way the Standard model (SM) particles couple to axions is through the axion-photon chiral anomaly, characterized by the coupling parameter $g_{a\gamma\gamma}$, which is known to modify electrodynamics. Recently the modifications have been expanded to include two other axion-photon anomaly coupling parameters, g_{aEM} and g_{aMM}, which occur if magnetic monopoles exist at high energy, as suggested by the theory of quantum electromagnetodynamics (QEMD) [12–14].

Axion searches typically target the Kim-Shifman-Vainshtein-Zakharov (KSVZ) [4,5] and the Dine-Fischler-Srednicki-Zhitnitsky (DFSZ) [6,7] models, where $g_{a\gamma\gamma} = C_{a\gamma\gamma}\alpha/(2\pi f_a)$. Here f_a is the high-energy scale below the PQ symmetry is broken, with the axion mass given by $m_a \sim 5.7(10^{15}\ \mathrm{GeV}/f_a)$ neV [15], where α is the fine structure constant, and $C_{a\gamma\gamma} \sim 0.75$ or -1.92 for the DFSZ and the KSVZ models, respectively. If the PQ symmetry is broken before inflation, light axions can constitute the whole of dark matter, where mass values of m_a between (0.1–100) neV correspond to values of f_a near the grand unified theory scale (GUT-scale).

In this work we investigate the sensitivity of a high-voltage capacitor to g_{aEM} and g_{aMM} couplings inferred from the resulting axion modified electrodynamics, and conceive viable ways to search for axion dark matter and effects of high-energy monopoles at the GUT-scale. Our new proposals could significantly add to the current proposed experimental programs that search for GUT-scale axions via $g_{a\gamma\gamma}$ [16–32]. Here the primary function of the capacitor is to generate a background electric field to gain sensitivity to g_{aEM} and g_{aMM} through an axion generated oscillating electric and magnetic field respectively, which is different to experiments that search for $g_{a\gamma\gamma}$ through electric sensing with a background magnetic field, which have been proposed previously [23,33–36].

II. AXION-MONOPOLE MODIFIED ELECTRODYNAMICS WITH A STATIC BACKGROUND ELECTRIC FIELD

The axion is a pseudoscalar postulated to account for the dark matter halo of our galaxy. Correspondingy, its velocity dispersion is determined by the galactic virial velocity, $v_a \sim 10^{-3}$, implying a macroscopic de Broglie wave length, $\lambda_{\mathrm{dB}} = 2\pi/(m_a v_a) \simeq 10^3\ \mathrm{km}(\mathrm{neV}/m_a)(10^{-3}/v_a)$.

*michael.tobar@uwa.edu.au

Therefore, axion dark matter behaves as an approximately spatially homogeneous and monochromatic classical field, which oscillates with a frequency determined by the axion mass, $\omega_a \simeq m_a$, and an amplitude proportional to the square root of the energy density of DM in the galactic halo, $\rho_{\rm DM} \simeq 0.45\ {\rm GeV/cm^3}$,

$$a(t,\vec{r}) \simeq \sqrt{2\rho_{\rm DM}}\cos(m_a t)/m_a. \tag{1}$$

The generalized axion electrodynamics equations, expanded to include the axion field and the extra coupling terms, g_{aMM} and g_{aEM}, in addition to the conventional $g_{a\gamma\gamma}$ term, are given by [13,14,37–39] (SI units)

$$\vec{\nabla}\cdot\vec{E}_1 = g_{a\gamma\gamma}c\vec{B}_0\cdot\vec{\nabla}a - g_{aEM}\vec{E}_0\cdot\vec{\nabla}a + \epsilon_0^{-1}\rho_{e1}, \tag{2}$$

$$\begin{aligned}\mu_0^{-1}\vec{\nabla}\times\vec{B}_1 = {}& \epsilon_0\partial_t\vec{E}_1 + \vec{J}_{e1} + g_{a\gamma\gamma}c\epsilon_0(-\vec{\nabla}a\times\vec{E}_0 - \partial_t a\vec{B}_0)\\ & + g_{aEM}\epsilon_0(-\vec{\nabla}a\times c^2\vec{B}_0 + \partial_t a\vec{E}_0),\end{aligned} \tag{3}$$

$$\vec{\nabla}\cdot\vec{B}_1 = -\frac{g_{aMM}}{c}\vec{E}_0\cdot\vec{\nabla}a + g_{aEM}\vec{B}_0\cdot\vec{\nabla}a, \tag{4}$$

$$\begin{aligned}\vec{\nabla}\times\vec{E}_1 = {}& -\partial_t\vec{B}_1 + \frac{g_{aMM}}{c}(c^2\vec{\nabla}a\times\vec{B}_0 - \partial_t a\vec{E}_0)\\ & + g_{aEM}(\vec{\nabla}a\times\vec{E}_0 + \partial_t a\vec{B}_0),\end{aligned} \tag{5}$$

where $\vec{B}_0$ and $\vec{E}_0$ are the impressed background fields, generated from impressed free charge and current densities given by ρ_{e_0} and $\vec{J}_{e_0}$, respectively; $\vec{B}_1$ and $\vec{E}_1$ are the axion-induced fields, while ρ_{e1} and $\vec{J}_{e1}$ are the axion-induced charge and current densities.

We assume only a static background electric field so $\vec{B}_0 = 0$ and $\vec{J}_{e_0} = 0$, and ignore any possible axion modifications to the background fields. Then the background electric field is determined by the impressed charge density ρ_{e_0}, so

$$\vec{\nabla}\times\vec{E}_0 = 0, \qquad \vec{\nabla}\cdot\vec{E}_0 = \epsilon_0^{-1}\rho_{e_0}. \tag{6}$$

The axion field is strongly repelled by electric charges due to the infinite potential barrier, as has been discussed in Ref. [40] for the dual case of axions interacting with the magnetic charges through the coupling $g_{a\gamma\gamma}$. In particular, in the close r_0 vicinity of a charge, the axion field behaves as $a(r) \sim \exp(-r_0/r)$, where r is the radial coordinate associated to a given charge situated at $r = 0$. Thus, one has $a = 0$ at the locations of the charged particles [41] and therefore $\vec{\nabla}a \neq 0$ in the vicinity of r_0, irrespective of the details of the low-energy behavior of the axion field. Note that this gradient is directed along the electric field $\vec{E}_{0i}$ generated by a given ith particle. In contrast, when $r \gg r_0$, the axion field is determined fully by the background, so that $\vec{\nabla}a \sim 0$, due to the small $v_a \sim 10^{-3}$ velocities of the DM axions. Thus, importantly in this case one can determine that $\vec{E}_0\cdot\vec{\nabla}a = \vec{\nabla}\cdot(a\vec{E}_0)$, since the product of $a(\vec{\nabla}\cdot\vec{E}_0) = 0$ for all values of r due to the effect described above. Also, since $\vec{\nabla}a$ is along the direction of the electric field, we may conclude $\vec{\nabla}a\times\vec{E}_0 = 0$. In this case, the axion Maxwell equations (2)–(5) with only a static background electric field, become

$$\vec{\nabla}\cdot(\vec{E}_1 + g_{aEM}a\vec{E}_0) = \epsilon_0^{-1}\rho_{e1}, \tag{7}$$

$$\mu_0^{-1}\vec{\nabla}\times\vec{B}_1 = \epsilon_0\partial_t(\vec{E}_1 + g_{aEM}a\vec{E}_0) + \vec{J}_{e1}, \tag{8}$$

$$\vec{\nabla}\cdot\left(\vec{B}_1 + \frac{g_{aMM}a\vec{E}_0}{c}\right) = 0, \tag{9}$$

$$\vec{\nabla}\times\vec{E}_1 = -\partial_t\left(\vec{B}_1 + \frac{g_{aMM}a\vec{E}_0}{c}\right). \tag{10}$$

Consequently the effect of DM axions can be described by means of an effective polarization and magnetization [42] ($\vec{P}_1$ from g_{aEM}, and $\vec{M}_1$ from g_{aMM}) in the regions where $\vec{E}_0 \neq 0$, both proportional to E_0, and given by

$$\vec{P}_1 = g_{aEM}a\epsilon_0\vec{E}_0, \tag{11}$$

$$\vec{M}_1 = -g_{aMM}ac\epsilon_0\vec{E}_0. \tag{12}$$

This means one can rewrite the Eqs. (7)–(10) as follows:

$$\vec{\nabla}\cdot\vec{D}_1 = \rho_{e1}, \tag{13}$$

$$\mu_0^{-1}\vec{\nabla}\times\vec{B}_1 = \partial_t\vec{D}_1 + \vec{J}_{e1}, \tag{14}$$

$$\vec{\nabla}\cdot\vec{H}_1 = 0, \tag{15}$$

$$\vec{\nabla}\times\vec{E}_1 = -\mu_0\partial_t\vec{H}_1, \tag{16}$$

where the effective auxiliary fields may be defined in vacuo as

$$\vec{D}_1 = \epsilon_0\vec{E}_1 + \vec{P}_1, \tag{17}$$

$$\vec{H}_1 = \mu_0^{-1}\vec{B}_1 - \vec{M}_1. \tag{18}$$

In this work we implement Poynting theorem to calculate the sensitivity of the proposed haloscope. In electrodynamics there are at least four Poynting vectors that may be realized, which over the years lead to the Abraham-Minkowski-Poynting theorem controversy [43]. In this case since the curl of $\vec{M}_1$ is zero, then from (18), $\vec{\nabla}\times\vec{H}_1 = \frac{1}{\mu_0}\vec{\nabla}\times\vec{B}_1$. Thus, when the background field is a

static electric field, the analogous Abraham ($\vec{E}_1 \times \vec{H}_1$) and Minkowski-Poynting vectors ($\frac{1}{\epsilon_0\mu_0}\vec{D}_1 \times \vec{B}_1$) are equal [36], so for the case of the static electric background any of the four Poynting theorems will give the same result.

A. Harmonic equations in phasor form

To solve for harmonic solutions the implementation of the phasor form of Maxwell's equations is a common technique. Here we develop the phasor form of the modified axion electrodynamics. First, the axion pseudoscalar $a(t)$ may be written as $a(t) = \frac{1}{2}(\tilde{a}e^{-j\omega_a t} + \tilde{a}^* e^{j\omega_a t}) = \mathrm{Re}(\tilde{a}e^{-j\omega_a t})$, and thus, in phasor form and in the frequency domain, $\tilde{A} = \tilde{a}e^{-j\omega_a t}$ and $\tilde{A}^* = \tilde{a}^* e^{j\omega_a t}$. In contrast, the electric and magnetic fields as well us the electric current are represented as vector phasors. For example, we set $\vec{B}_1(\vec{r},t) = \frac{1}{2}(\mathbf{B}_1(\vec{r})e^{-j\omega_1 t} + \mathbf{B}_1^*(\vec{r})e^{j\omega_1 t}) = \mathrm{Re}[\mathbf{B}_1(\vec{r})e^{-j\omega_1 t}]$, so we define the vector phasor (bold) and its complex conjugate by $\tilde{\mathbf{B}}_1(\vec{r},t) = \mathbf{B}_1(\vec{r})e^{-j\omega_1 t}$ and $\tilde{\mathbf{B}}_1^*(\vec{r},t) = \mathbf{B}_1^*(\vec{r})e^{j\omega_1 t}$, respectively. Following these definitions, the axion modified Ampere's law in (8), and Faraday's law in (10), in phasor form become

$$\begin{aligned}\frac{1}{\mu_0}\vec{\nabla}\times\mathbf{B}_1 &= \mathbf{J}_{e1} - j\omega_1\epsilon_0\mathbf{E}_1 - j\omega_a g_{aEM}\epsilon_0\tilde{a}\vec{E}_0,\\ \frac{1}{\mu_0}\vec{\nabla}\times\mathbf{B}_1^* &= \mathbf{J}_{e1}^* + j\omega_1\epsilon_0\mathbf{E}_1^* + j\omega_a g_{aEM}\epsilon_0\tilde{a}^*\vec{E}_0,\end{aligned} \tag{19}$$

$$\begin{aligned}\vec{\nabla}\times\mathbf{E}_1 &= j\omega_1\mathbf{B}_1 + j\frac{\omega_a g_{aMM}}{c}\tilde{a}\vec{E}_0,\\ \vec{\nabla}\times\mathbf{E}_1^* &= -j\omega_1\mathbf{B}_1^* - j\frac{\omega_a g_{aMM}}{c}\tilde{a}^*\vec{E}_0.\end{aligned} \tag{20}$$

In the following subsections we implement Poynting theorem to and apply it to haloscopes in the reactive regime, well below any resonant frequencies.

1. Complex Poynting theorem

To implement Poynting theorem to calculate the sensitivity of a reactive system, we need to calculate the imaginary power flow, in a lossless system. For reactive systems the real term can be ignored [36], and conversely for resonant systems it is the real power that dominates and the reactive power is ignored. The complex Poynting vector and its complex conjugate are defined by

$$\mathbf{S}_1 = \frac{1}{2\mu_0}\mathbf{E}_1\times\mathbf{B}_1^* \quad \text{and} \quad \mathbf{S}_1^* = \frac{1}{2\mu_0}\mathbf{E}_1^*\times\mathbf{B}_1, \tag{21}$$

where $\mathbf{S}_1$ is the complex power density of the harmonic electromagnetic wave or oscillation, with the real part equal to the time averaged power density and the imaginary term equal to the reactive power, which may be inductive (magnetic energy dominates) or capacitive (electrical energy dominates). Unambiguously we may calculate the imaginary part of the Poynting vector by

$$j\mathrm{Im}(\mathbf{S}_1) = \frac{1}{2}(\mathbf{S}_1 - \mathbf{S}_1^*). \tag{22}$$

Taking the divergence of Eq. (22) we find

$$j\vec{\nabla}\cdot\mathrm{Im}(\mathbf{S}_1) = \frac{1}{2}\vec{\nabla}\cdot(\mathbf{S}_1 - \mathbf{S}_1^*) \tag{23}$$

with

$$\begin{aligned}\vec{\nabla}\cdot\mathbf{S}_1 &= \frac{1}{2}\vec{\nabla}\cdot\left(\mathbf{E}_1\times\frac{1}{\mu_0}\mathbf{B}_1^*\right)\\ &= \frac{1}{2\mu_0}\mathbf{B}_1^*\cdot\vec{\nabla}\times\mathbf{E}_1 - \mathbf{E}_1\cdot\frac{1}{2\mu_0}\vec{\nabla}\times\mathbf{B}_1.\end{aligned} \tag{24}$$

For the reactive solution, $\omega_a = \omega_1$, and substituting Eqs. (19) and (20) into Eq. (24) and it complex conjugate leads to

$$\begin{aligned}\vec{\nabla}\cdot\mathbf{S}_1 = {}& \frac{j\omega_a\epsilon_0}{2}(c^2\mathbf{B}_1^*\cdot\mathbf{B}_1 - \mathbf{E}_1\cdot\mathbf{E}_1^*) - \frac{1}{2}\mathbf{E}_1\cdot\mathbf{J}_{e1}^*\\ & - \frac{j\omega_a\epsilon_0 g_{aEM}}{2}\mathbf{E}_1\cdot\tilde{a}^*\vec{E}_0 + \frac{j\omega_a\epsilon_0 c g_{aMM}}{2}\mathbf{B}_1^*\cdot\tilde{a}\vec{E}_0,\end{aligned} \tag{25}$$

$$\begin{aligned}\vec{\nabla}\cdot\mathbf{S}_1^* = {}& \frac{j\omega_a\epsilon_0}{2}(\mathbf{E}_1\cdot\mathbf{E}_1^* - c^2\mathbf{B}_1^*\cdot\mathbf{B}_1) - \frac{1}{2}\mathbf{E}_1^*\cdot\mathbf{J}_{e1}\\ & + \frac{j\omega_a\epsilon_0 g_{aEM}}{2}\mathbf{E}_1^*\cdot\tilde{a}\vec{E}_0 - \frac{j\omega_a\epsilon_0 c g_{aMM}}{2}\mathbf{B}_1\cdot\tilde{a}^*\vec{E}_0.\end{aligned} \tag{26}$$

The phase of the axion is not an observable, and is arbitary, so setting $a_0 = \tilde{a} = \tilde{a}^*$ and by substituting (25) and (26) into (23), as well as realizing any induced dissipative electrical currents $\mathbf{J}_{e1}$ are proportional to the induced electric fields, $\mathbf{E}_1$ we find

$$\begin{aligned}\vec{\nabla}\cdot\mathrm{Im}(\mathbf{S}_1) = {}& \frac{\omega_a\epsilon_0}{2}(c^2\mathbf{B}_1^*\cdot\mathbf{B}_1 - \mathbf{E}_1\cdot\mathbf{E}_1^*)\\ & - \frac{\omega_a\epsilon_0 a_0}{4}(g_{aEM}(\mathbf{E}_1^* + \mathbf{E}_1)\\ & + g_{aMM}c(\mathbf{B}_1^* + \mathbf{B}_1))\cdot\vec{E}_0.\end{aligned} \tag{27}$$

Then applying the divergence theorem, we obtain

$$\begin{aligned}\frac{\oint\mathrm{Im}(\mathbf{S}_1)\cdot\hat{n}ds}{\omega_a} = {}& \frac{\epsilon_0}{2}\int\Big((c^2\mathbf{B}_1^*\cdot\mathbf{B}_1 - \mathbf{E}_1\cdot\mathbf{E}_1^*)\\ & - \frac{a_0}{2}(g_{aEM}(\mathbf{E}_1^* + \mathbf{E}_1)\\ & - g_{aMM}c(\mathbf{B}_1^* + \mathbf{B}_1))\cdot\vec{E}_0\Big)dv.\end{aligned} \tag{28}$$

If we assume all external reactive sources and sinks are zero, $[\mathrm{Im}(\mathbf{S}_1) \sim 0]$ then the reactive power is only supplied by the axion mixing with the static back ground fields, then the reactive stored energy in the circuit may be written as

$$U_1 = \frac{\epsilon_0}{2}\int((c^2\mathbf{B}_1^*\cdot\mathbf{B}_1 - \mathbf{E}_1\cdot\mathbf{E}_1^*))dv = \frac{\epsilon_0 a_0}{4}\int(g_{aEM}(\mathbf{E}_1^*+\mathbf{E}_1) - g_{aMM}c(\mathbf{B}_1^*+\mathbf{B}_1))\cdot\vec{E}_0 dv, \tag{29}$$

where a negative stored energy is capacitive, and a positive stored energy is inductive. Finally from (29), by squaring the last term and dividing by the second term, we may show that the stored energy may also be expressed as

$$U_1 = \frac{\epsilon_0 a_0^2(\int(g_{aEM}(\mathbf{E}_1^*+\mathbf{E}_1) - g_{aMM}c(\mathbf{B}_1^*+\mathbf{B}_1))\cdot\vec{E}_0 dv)^2}{8\int((c^2\mathbf{B}_1^*\cdot\mathbf{B}_1 - \mathbf{E}_1\cdot\mathbf{E}_1^*))dv}. \tag{30}$$

III. HIGH-VOLTAGE CAPACITOR: SENSITIVITY TO AXION-MONOPOLE COUPLINGS

A. Axion-induced electric field

A high-voltage capacitor excited with a static electric background field has been shown to be proportionally sensitive to scalar field dark matter, $\phi(t)$, in the low-mass limit, through the dimensionful coupling constant $g_{\phi\gamma\gamma}$ [38,44]. For resonant haloscopes, the sensitivity to the axion pseudoscalar field $a(t)$ through the coupling parameter g_{aEM}, has been shown to give the same limit as $g_{\phi\gamma\gamma}$ for scalar-field dark matter [37]. Thus, it was hypothesized that a high-voltage capacitor may also be sensitive to g_{aEM} in the low-mass limit, and here we show that this is indeed true, with the axion dark matter modification to electrodynamics also appearing as an effective polarization.

From Maxwell electrodynamics it is straightforward to show that the electric field vector phasor inside a cylindrical parallel-plate capacitor may be written as [45]

$$\tilde{\mathbf{E}}_1 = \tilde{E}_{01}J_0\left(\frac{\omega_a}{c}r\right)e^{-j\omega_a t}\hat{z}, \qquad \tilde{E}_{01} = \frac{\tilde{q}_1}{\epsilon_0\pi R_c^2} = \frac{\tilde{\sigma}_1}{\epsilon_0}, \tag{31}$$

and then to confirm the magnetic-field vector phasor as

$$\tilde{\mathbf{B}}_1 = -j\frac{\tilde{E}_{01}}{c}J_1\left(\frac{\omega_a}{c}r\right)e^{-j\omega_a t}\hat{\varphi}. \tag{32}$$

From the series expansion of (31) and (32), in the quasistatic limit when the Compton wavelength is large compared to the size of the capacitor (as $\omega_a \to 0$), the magnetic and electric field phasor amplitudes become

$$\mathbf{E}_1 \approx \tilde{E}_{01}\hat{z}, \qquad \mathbf{B}_1 \approx -j\tilde{E}_{01}\frac{r\omega_a}{2c^2}\hat{\varphi}, \tag{33}$$

assuming the electric field is in phase and the magnetic field is out of phase. Given that $\mathbf{B}_1$ is imaginary and $\mathbf{E}_1$ is real, Eq. (30) for this experiment becomes,

$$U_1 = \frac{g_{aEM}^2 a_0^2\epsilon_0(\int\mathbf{E}_1\cdot\vec{E}_0 dv)^2}{2\int((c^2\mathbf{B}_1^*\cdot\mathbf{B}_1 - \mathbf{E}_1\cdot\mathbf{E}_1^*))dv}, \tag{34}$$

which by substituting (31) and (32) into (34) gives

$$U_1 = -g_{aEM}^2 a_0^2\epsilon_0 E_0^2 V c\frac{c}{2\pi R_c}\frac{J_1\left(\frac{\omega_a}{c}r\right)}{J_0\left(\frac{\omega_a}{c}r\right)}, \tag{35}$$

where $v_c = \pi R_c^2 d_c$ is the volume of the capacitor. Then, given that $a_0^2 = 2\langle a_0\rangle^2$, in the quasistatic limit ($\omega_a \to 0$), the first term of the expansion of (35) in powers of ω_a is a constant term given by

$$U_1 = -g_{aEM}^2\langle a_0\rangle^2\epsilon_0 E_0^2\pi R_c^2 d_c. \tag{36}$$

The negative sign just indicates the reactive power delivered to the capacitor is negative. Equating the magnitude of (36) to the stored energy in the capacitor $|U_1| = \frac{1}{2}\tilde{V}_1\tilde{V}_1{}^* C_a = \langle V_1\rangle^2 C_a$, the rms voltage across the capacitor may be calculated as

$$\langle V_1\rangle = g_{aEM}\langle a_0\rangle V_0, \quad \text{where } V_0 = E_0 d_c, \quad \text{so } \langle E_{01}\rangle = g_{aEM}\langle a_0\rangle E_0, \tag{37}$$

with a schematic of experiment shown in Fig. 1. This is very similar to the proposal to search for the $g_{\phi\gamma\gamma}$ coupling to scalar dark matter [44].

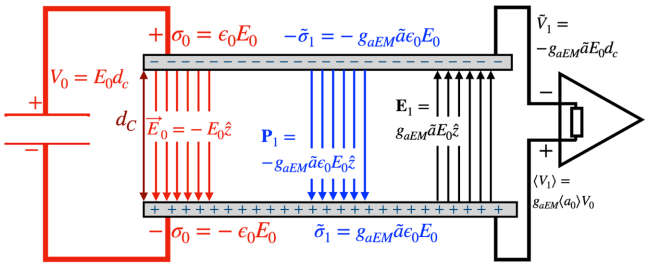

FIG. 1. Schematic of the proposed experiment, with the capacitor of volume $v_c = \pi R_c^2 d_c$, charged by a high voltage, V_0, which produces a static electric field, $\vec{E}_0$, inside the capacitor. Putative axion dark matter interacts with the static field and creates an effective polarization (10) oscillating between the plates, which is discontinuous at the plate boundaries. This produces an alternating voltage measured with the aid of a low noise high-impedance amplifier.

In the quasi static limit, when $\omega_a^2 < \frac{1}{L_1 C_1}$, the electrical stored energy is much greater than the magnetic, so (34) becomes

$$U_1 \approx -\frac{g_{aEM}^2 a_0^2 \epsilon_0 (\int \mathbf{E}_1 \cdot \vec{E}_0 dv)^2}{2 \int \mathbf{E}_1 \cdot \mathbf{E}_1^* dv}. \quad (38)$$

Then substituting in the approximate quasi static electric field from (33) into (38), we may also derive (36).

The observable for this experiment is the oscillating output voltage, given by

$$\langle V_1 \rangle = \mathcal{K}_{V_{\rm EM}} g_{aEM} \langle a_0 \rangle, \quad \text{where } \mathcal{K}_{V_{\rm EM}} = V_0, \quad (39)$$

and $\mathcal{K}_{V_{\rm EM}}$ is the transduction strength from the effective dimensionless axion field ($\theta_{0_{\rm EM}} = g_{aEM} a_0$) to volts [46]. The spectral noise density, S_V, associated with the readout can be measured in units volts squared per Hz, so that the square root spectral density of noise referred to the effective dimensionless axion field may be written as

$$\sqrt{S_{\theta_{\rm EM}}} = \frac{\sqrt{S_V}}{|\mathcal{K}_{V_{\rm EM}}|}. \quad (40)$$

For cold dark matter the signal may be approximated as a narrow band noise source of line width Δf_a, which is equivalent to an effective Q-factor of $Q_a = \frac{f_a}{\Delta f_a}$. So the signal coherence time is given by, $\tau_a = \frac{Q_a}{f_a} = \frac{1}{\Delta f_a}$. In this case, the signal to noise ratio of the experiment is given by

$$SNR \sim \frac{\mathcal{K}_{V_{\rm EM}} g_{aEM} \langle a_0 \rangle}{\sqrt{S_V}} (t\tau_a)^{\frac{1}{4}} = \frac{\langle \theta_{0_{\rm EM}} \rangle}{\sqrt{S_{\theta_{\rm EM}}}} (t\tau_a)^{\frac{1}{4}}, \quad (41)$$

for a measurement time $t > \tau_a$; if $t < \tau_a$, we may substitute $(t\tau_a)^{\frac{1}{4}} \to t^{\frac{1}{2}}$, and we use these equations to estimate the sensitivity of this experiment.

B. Axion-induced magnetic field coupled to a magnetic circuit

The static electric field produced by the high-voltage capacitor will also interact with the axion to create an oscillating magnetic flux density, $\vec{B}_1$, through g_{aMM}. To readout $\vec{B}_1$, we may couple the high-voltage capacitor to a magnetic circuit as shown in Fig. 2. The magnetic circuit improves the sensitivity in two ways. First, without the magnetic circuit, the axion-induced magnetic field inside and outside the capacitor would be in opposite directions, while the static background electric field will be all in the same direction. This would potentially cause cancellation equivalent to a reduced form factor due to the reduction of the value of $\int \mathbf{B}_1 \cdot \vec{E}_0 dv$. Secondly, without the magnetic circuit the magnetomotive force (mmf) produced by the effective magnetization, $\mathcal{F}_1 = \int_0^{d_c} \vec{M}_1 \cdot \vec{dl} = g_{aMM} a c \epsilon_0 E_0 d_c$,

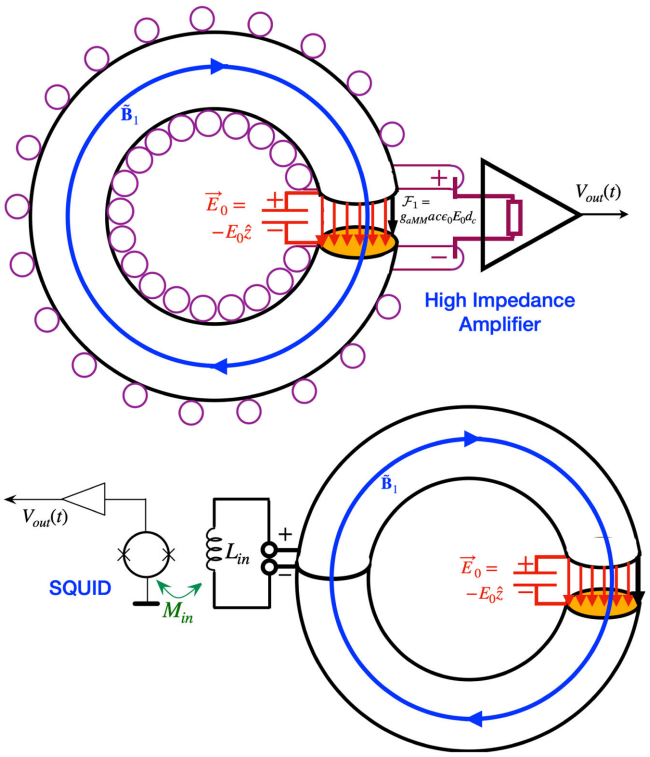

FIG. 2. Schematic of proposed experiments, with a lossless capacitor of volume $v_c = \pi R_c^2 d_c$ charged by a high voltage and coupled to a toroidal magnetic circuit. The axion interacting with the static electric field produces an oscillating mmf, which generates an oscillating magnetic flux throughout the magnetic circuit. Top, a large winding output read out by a high-impedance amplifier (HIA). Bottom, a single winding pick up coil readout by a low impedance SQUID amplifier.

will create a significantly reduced $\vec{B}_1$, because the demagnetization field, $\vec{H}_1$, acts in the opposite direction ($\vec{M}_1 = \mu_0^{-1} \vec{B}_1 - \vec{H}_1$). Creating a transformer like magnetic circuit readout means the demagnetization field becomes insignificant ($\vec{H}_1 \to 0$), so with proper design $\vec{B}_1 = \mu_0 \vec{M}_1$ within the capacitor.

To construct a low-noise readout two approaches may be undertaken as highlighted previously in [23]. The first is to couple to a single loop readout coil, to minimize the readout output impedance and maximize magnetic-circuit reluctance, and use a SQUID amplifier in the first stage. The second is to couple to a high-inductance coil with multiple windings and readout with a high-impedance amplifier in the first stage. The former naturally measures current or flux with a low-impedance output, while the latter measures induced voltage with a high-impedance output. In both cases we can classify the readouts as impedance mismatch, with the sensitivity determined by the reactive power flow in the circuit.

Assuming the magnetic field is in phase and the induced electric field is out of phase, then we set $\mathbf{B}_1$ as

real and $\mathbf{E}_1$ as imaginary, and Eq. (30) for this experiment becomes

$$U_1 = \frac{\left(\frac{g_{aMM}a_0\epsilon_0 c}{2}\int \mathbf{B}_1 \cdot \vec{E}_0 dv\right)^2}{\int\left(\frac{1}{2\mu_0}\mathbf{B}_1^* \cdot \mathbf{B}_1 - \frac{\epsilon_0}{2}\mathbf{E}_1 \cdot \mathbf{E}_1^*\right)dv}. \tag{42}$$

In the quasistatic limit, when $\omega_a^2 < \frac{1}{L_1 C_1}$, the magnetic stored energy is much greater than the electric, so (42) may be approximated as

$$U_1 \approx \frac{g_{aMM}^2 a_0^2 \epsilon_0}{2}\frac{(\int \mathbf{B}_1 \cdot \vec{E}_0 dv)^2}{\int \mathbf{B}_1^* \cdot \mathbf{B}_1 dv}. \tag{43}$$

The magnetic-flux density-phasor amplitude is of the form $\mathbf{B}_1 \approx -\tilde{B}_{01}e^{-j\omega_a t}\hat{\phi}$, and substituting into (43) we find that,

$$U_1 = g_{aMM}^2\langle a_0\rangle^2 \epsilon_0 E_0^2 \pi R_c^2 d_c. \tag{44}$$

Equating the stored energy in (44) with $\frac{1}{\mu_0}\langle B_{01}\rangle^2 v_c$, the rms amplitude of the magnetic field may be shown to be

$$\langle B_{01}\rangle = g_{aMM}\langle a_0\rangle \frac{E_0}{c}. \tag{45}$$

The voltage across the coil is simply given by Faraday's law, $\tilde{V}_1 = -N_t|\partial_t \mathbf{B}_1|\pi R_c^2$, so that the rms output voltage is given by

$$\langle V_1\rangle = g_{aMM}\langle a_0\rangle N_t\left(\frac{\omega_a \pi R_c^2}{d_c c}\right)V_0, \tag{46}$$

where N_t is the number of turns around the toroidal coil. For the toroidal coil with multiple turns coupled to the high-impedance amplifier, the inductance is given by

$$L_t = \frac{\mu_r\mu_0 N_t^2 \pi R_c^2}{2\pi r_t - d_c}, \tag{47}$$

where r_t the radius to the midpoint of the toroid. For the low-impedance output coupled to the SQUID amplifier, the inductance of the single pick up coil is given by

$$L_t \approx \mu_0\mu_r R_s\left[\ln\left(\frac{8R_c}{r_w}\right) - \frac{7}{4}\right], \tag{48}$$

where we assume the coil has a radius R_c, and r_w is the radius of the coil wire. The Thevenin equivalent circuit is shown in Fig. 3.

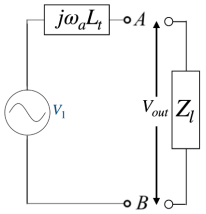

FIG. 3. Thevenin equivalent circuit at the readout coil of the magnetic circuit shown in Fig. 2. The load impedance Z_l is mainly determined by the input impedance of the SQUID or high-impedance amplifier.

1. High-impedance output

The high-impedance output requires a large inductance as shown in Fig. 2, this is because the rms value of the axion-induced voltage, in (46), is proportional to N_t, while the inductance, in (47), L_t, is proportional to N_t^2. The limit on the value of L_t is set, so it is at least an order of magnitude lower than the input impedance of the high-impedance amplifier that reads out the voltage. Typically a high-impedance amplifier has an input impedance of order 10 MΩ [44], so this gives the restriction of the inductance of the toroid depending on the highest frequency of interest. Assuming $\omega_a L_t < 10$ MΩ, with the rms voltage in (46) as the observable, we may define the transduction strength as

$$\mathcal{K}_{V_{MM}} = N_t\left(\frac{\omega_a \pi R_c^2}{d_c c}\right)V_0, \tag{49}$$

so in a similar way to (41), the signal to noise ratio is given by

$$SNR \sim \frac{\mathcal{K}_{V_{MM}} g_{aMM}\langle a_0\rangle}{\sqrt{S_V}}(t\tau_a)^{\frac{1}{4}} = \frac{\langle\theta_{0_{MM}}\rangle}{\sqrt{S_{\theta_{MM}}}}(t\tau_a)^{\frac{1}{4}}, \tag{50}$$

where $\sqrt{S_{\theta_{MM}}} = \frac{\sqrt{S_V}}{|\mathcal{K}_{V_{MM}}|}$.

2. Low-impedance output

For the low-impedance output we configure the readout with a SQUID amplifier as shown in Fig. 2. In this case the observable can be thought of as magnetic flux created by the axion and picked up by the pick up coil, which senses the induced current. In this case the impedance of the pickup coil should be minimized, so is best realized with a single loop. The rms magnetic flux induced by the axion in the magnetic circuit is given by

$$\langle\Phi_a\rangle = g_{aMM}\langle a_0\rangle \frac{E_0 \pi R_c^2}{c}. \tag{51}$$

The pickup coil of inductance given by (48), links to the SQUID through a mutual inductance, M_{in} via a SQUID input coil of inductance L_{in}, so the SQUID amplifier senses the following magnetic flux,

$$\langle\Phi_{\text{SQ}}\rangle = \frac{M_{\text{in}}}{L_t + L_{\text{in}}}\langle\Phi_a\rangle, \tag{52}$$

where, Φ_{SQ} is our observable so the transduction may be defined as

$$\mathcal{K}_{\Phi_{MM}} = \frac{M_{\rm in}}{L_t + L_{\rm in}} \frac{\pi R_c^2}{c d_c} V_0, \tag{53}$$

and in a similar way to (41), the signal to noise ratio is given by

$$SNR \sim \frac{\mathcal{K}_{\Phi_{MM}} g_{aMM} \langle a_0 \rangle}{\sqrt{S_{\Phi_{SQ}}}} (t\tau_a)^{\frac{1}{4}} = \frac{\langle \theta_{0_{MM}} \rangle}{\sqrt{S_{\theta_{MM}}}} (t\tau_a)^{\frac{1}{4}}, \tag{54}$$

where $\sqrt{S_{\theta_{MM}}} = \frac{\sqrt{S_{\Phi_{SQ}}}}{|\mathcal{K}_{\Phi_{MM}}|}$.

IV. PROJECTED SENSITIVITIES

For the GUT-scale axion the frequencies of interest are considered to be between 24 kHz to 24 MHz, equivalent to an axion mass range between 10^{-10} eV to 10^{-7} eV. For the purpose of these calculations we restrict ourselves to the frequency range between 2.4 kHz to 2.4 MHz (between 10^{-11} eV to 10^{-8} eV), suitable for the components of the experiment, and still overlapping much of the GUT-scale mass range. For example, many lumped element components do not work well in the MHz range and the low-loss permeable material is only specified up to these frequencies. The experiment will have sensitivity above 2.4 MHz, but it is harder to predict without building, characterizing, and calibrating properly at higher frequencies, thus conservatively we just show limits up to 2.4 MHz.

The experiment may be configured to probe simultaneously g_{aMM} and g_{aEM} by implementing together one of the magnetic circuit readouts to measure the axion-induced oscillating magnetic field in (45) and the high-impedance output to measure the axion-induced electric field in (37) respectively. Note a limit on g_{aEM} would also give a limit on the scalar-field dark matter parameter $g_{\phi\gamma\gamma}$ at the same time [44].

One can envisage undertaking this experiment with cylindrical oxygen-free copper capacitor plates in vacuum. Oxygen-free copper has been shown to be able to withstand impulses of electric fields of up to 200 MV/m in vacuum [47]. Combining this with the availability of commercially available 600 kV power supplies [44] means that a capacitor plate of 10 cm radius and 0.5 cm separation, would have an electric field of 120 MV/m between the capacitor plates, with a capacitance of 56 pF. During this work we envisage using such a capacitor cooled to 4 K, with a high-impedance amplifier readout over a frequency range of 2.4 kHz to 2.4 MHz, so the impedance of the capacitor would remain about an order of magnitude lower than the input impedance of the low noise high-impedance amplifier, which is of the order of 10 MΩ [44]. Such amplifiers have been shown to have a very low noise spectrum at 4 Kelvin, of order

$$\sqrt{S_V} = \sqrt{\frac{7.4185 \times 10^{-14}}{f^{1.12}} + \frac{9.252 \times 10^{-19}}{f^{0.176}}} \mathrm{V}/\sqrt{\mathrm{Hz}}, \tag{55}$$

where f is the Fourier frequency offset in Hz, where we search for the axion at $f = \frac{\omega_a}{2\pi}$.

For the magnetic circuit readout we assume a toroid with a low permittivity core of 14; molypermalloy powder can be used to realize such a core, with efficiency over the frequency range of interest. For the purposes of estimating the sensitivity in a tabletop experiment, we assume a 10 cm scale experiment, with the toroid cross section radius equal to the radius of the capacitor, $R_c = 10$ cm. Assuming an average toroidal radius of 45 cm (similar size to ABRACADABRA 10 cm), we can set the number of turns for the high-impedance output to about 600, so the inductance of the toroid would be, $L_t = 70$ mH, giving a maximum impedance of 1 MΩ at 2.4 MHz. This circuit could be readout with a similar high-impedance amplifier with the noise spectrum given by (55).

For the low impedance magnetic circuit readout we want to minimize the inductance, which can be achieved by choosing a relatively thick wire in a single turn pick up coil. If we use a 5 mm radius wire, the inductance of the pick up coil can be calculated to be $L_t = 5.8$ μH. To calculate the noise introduced by the SQUID amplifier, we assume we may reproduce the excellent noise properties of the SHAFT experiment [22], which we convert to flux noise, and fit to give [46],

$$\sqrt{S_{\phi_{SQ}}} \sim \Phi_0 \times 10^{-6} \sqrt{0.688 + \frac{1.76 \times 10^{30}}{f^8} + 3.48 \times 10^{-26} f^4} \ \mathrm{Wb}/\sqrt{\mathrm{Hz}}, \tag{56}$$

where $\Phi_0 = \frac{h}{2e} = 2.0678 \times 10^{-15}$ Wb is the magnetic flux quantum. Typical SQUID parameters set $M_{\rm in} \sim 8$ nH and $L_{\rm in} \sim 150$ nH [22,23], which we use in our sensitivity calculations.

There may be a question on how the low-noise readouts perform in the presence of such a large, applied DC voltage and electric field. First, the SQUID and high-impedance amplifier circuits that readout and search for g_{aMM} couplings may be electrically isolated from the high voltage and fields, as a nonconducting element may be place between the magnetic circuit and capacitor plate, and the SQUID or high-impedance amplifier may be far away from the fringing electric fields. Secondly, the high-impedance amplifier that measures the AC electric field effects and searches for g_{aEM} couplings must be AC coupled, so the DC voltage is suppressed at the input, and it would have to be properly designed and characterized for the frequency

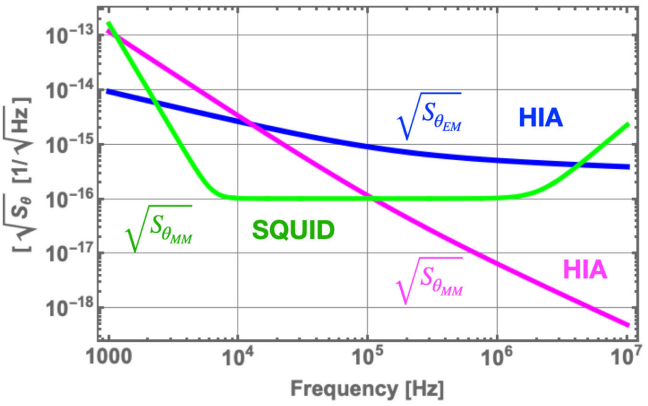

FIG. 4. Estimated spectral sensitivity for the three proposed detectors, from Eqs. (40), (50), and (54), using the assumed parameters given in the text.

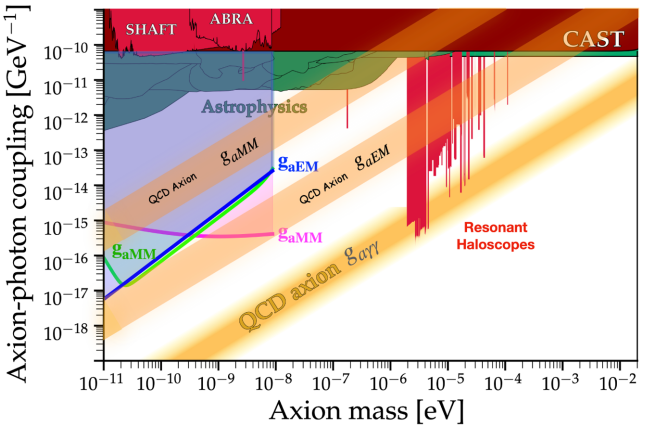

FIG. 5. Estimated order of magnitude sensitivity to axion-photon coupling parameters, g_{aEM} and g_{aMM}, for the three proposed detectors, derived from Eqs. (41), (50), and (54), with SNR set to unity, using the assumed parameters given in the text and with 18 days of continuous data taking. Note the resonant haloscopes [48–66], SHAFT [22], ABRA [20], and ADMX SLIC [16] are only sensitive to $g_{a\gamma\gamma}$ and not to g_{aMM} and g_{aEM}. The constraints from astrophysics and CAST hold for both the $g_{a\gamma\gamma}$ and the g_{aMM} couplings [13]. Moreover, CAST [67] has been shown to have sensitivity to $g_{\phi\gamma\gamma}$ and hence g_{aEM} [44]. The figure has been adapted from limits listed in Ref. [68].

range of interest. This situation can occur in ion-trapping experiments, for which the high-impedance amplifier was designed for, and should be able to be solved so an extremely sensitive search may be undertaken.

First we present the sensitivities in terms of the effective dimensionless axion spectral noise, which is independent of the axion signal and only depends on the transduction sensitivity and noise in the detector [46], and is plotted in Fig. 4. Following this, we assume that putative axions make up all of the galactic halo dark matter density, and present as a narrow band noise source due to virialization of dark matter within the halo. For this type of signal the signal to noise ratios are given by Eq. (41), (50), and (54), where the rms value of the effective dimensionless axion field is related to the dark matter density, $\rho_{\rm DM}$, by

$$\langle \theta_{0_i} \rangle = g_{ai} \frac{\sqrt{\rho_{\rm DM} c^3}}{\omega_a}, \tag{57}$$

where $i = MM$ or EM. The order of magnitude exclusion limits are set by assuming SNR $= 1$ and assuming the experiment runs for 18 days continuously, and are plotted in Fig. 5. From the plots we may conclude that these experiments can search for the GUT-scale QCD axion if putative heavy monopoles exist.

ACKNOWLEDGMENTS

This work was funded by the Australian Research Council Centre of Excellence for Engineered Quantum Systems, CE170100009 and the Australian Research Council Centre of Excellence for Dark Matter Particle Physics, CE200100008. A. V. S. is funded by the UK Research and Innovation Grant No. MR/V024566/1. A. R. acknowledges support by the Deutsche Forschungsgemeinschaft (DFG, German Research Foundation) under Germany's Excellence Strategy—EXC 2121 Quantum Universe—390833306 and under—491245950.

[1] R. D. Peccei and Helen R. Quinn, *CP* Conservation in the Presence of Pseudoparticles, Phys. Rev. Lett. **38**, 1440 (1977).
[2] F. Wilczek, Problem of Strong P and T Invariance in the Presence of Instantons, Phys. Rev. Lett. **40**, 279 (1978).
[3] Steven Weinberg, A New Light Boson?, Phys. Rev. Lett. **40**, 223 (1978).
[4] Jihn E. Kim, Weak-Interaction Singlet and Strong *CP* Invariance, Phys. Rev. Lett. **43**, 103 (1979).
[5] M. A. Shifman, A. I. Vainshtein, and V. I. Zakharov, Can confinement ensure natural *CP* invariance of strong interactions? Nucl. Phys. **B166**, 493 (1980).
[6] A. R. Zhitnitsky, On possible suppression of the axion hadron interactions. (In Russian), Sov. J. Nucl. Phys. **31**, 260 (1980).
[7] Michael Dine, Willy Fischler, and Mark Srednicki, A simple solution to the strong CP problem with a harmless axion, Phys. Lett. **104B**, 199 (1981).

[8] John Preskill, Mark B. Wise, and Frank Wilczek, Cosmology of the invisible axion, Phys. Lett. B **120**, 127 (1983).
[9] L. F. Abbott and P. Sikivie, A cosmological bound on the invisible axion, Phys. Lett. **120B**, 133 (1983).
[10] Michael Dine and Willy Fischler, The not-so-harmless axion, Phys. Lett. **120B**, 137 (1983).
[11] J. Ipser and P. Sikivie, Can Galactic Halos be Made of Axions?, Phys. Rev. Lett. **50**, 925 (1983).
[12] Daniel Zwanziger, Local-Lagrangian quantum field theory of electric, and magnetic charges, Phys. Rev. D **3**, 880 (1971).
[13] Anton V. Sokolov and Andreas Ringwald, Electromagnetic couplings of axions, arXiv:2205.02605.
[14] Anton V. Sokolov and Andreas Ringwald, Generic axion Maxwell equations: Path integral approach, arXiv:2303.10170.
[15] Giovanni Grilli di Cortona, Edward Hardy, Javier Pardo Vega, and Giovanni Villadoro, The QCD axion, precisely, J. High Energy Phys. 01 (2016) 034.
[16] N. Crisosto, P. Sikivie, N. S. Sullivan, D. B. Tanner, J. Yang, and G. Rybka, ADMX SLIC: Results from a Superconducting LC Circuit Investigating Cold Axions, Phys. Rev. Lett. **124**, 241101 (2020).
[17] Yonatan Kahn, Benjamin R. Safdi, and Jesse Thaler, Broadband and Resonant Approaches to Axion Dark Matter Detection, Phys. Rev. Lett. **117**, 141801 (2016).
[18] Jonathan L. Ouellet, Chiara P. Salemi, Joshua W. Foster, Reyco Henning, Zachary Bogorad, Janet M. Conrad, Joseph A. Formaggio, Yonatan Kahn, Joe Minervini, Alexey Radovinsky, Nicholas L. Rodd, Benjamin R. Safdi, Jesse Thaler, Daniel Winklehner, and Lindley Winslow, First Results from ABRACADABRA-10 cm: A Search for Sub-μeV Axion Dark Matter, Phys. Rev. Lett. **122**, 121802 (2019).
[19] Jonathan L. Ouellet, Chiara P. Salemi, Joshua W. Foster, Reyco Henning, Zachary Bogorad, Janet M. Conrad, Joseph A. Formaggio, Yonatan Kahn, Joe Minervini, Alexey Radovinsky, Nicholas L. Rodd, Benjamin R. Safdi, Jesse Thaler, Daniel Winklehner, and Lindley Winslow, Design and implementation of the ABRACADABRA-10 cm axion dark matter search, Phys. Rev. D **99**, 052012 (2019).
[20] Chiara P. Salemi, Joshua W. Foster, Jonathan L. Ouellet, Andrew Gavin, Kaliroë M. W. Pappas, Sabrina Cheng, Kate A. Richardson, Reyco Henning, Yonatan Kahn, Rachel Nguyen, Nicholas L. Rodd, Benjamin R. Safdi, and Lindley Winslow, Search for Low-Mass Axion Dark Matter with ABRACADABRA-10 cm, Phys. Rev. Lett. **127**, 081801 (2021).
[21] L. Brouwer *et al.*, Proposal for a definitive search for GUT-scale QCD axions, Phys. Rev. D **106**, 112003 (2022).
[22] Alexander V. Gramolin, Deniz Aybas, Dorian Johnson, Janos Adam, and Alexander O. Sushkov, Search for axion-like dark matter with ferromagnets, Nat. Phys. **17**, 79 (2021).
[23] Michael E. Tobar, Ben T. McAllister, and Maxim Goryachev, Broadband electrical action sensing techniques with conducting wires for low-mass dark matter axion detection, Phys. Dark Universe **30**, 100624 (2020).
[24] M. Goryachev, B. McAllister, and M. E. Tobar, Axion detection with precision frequency metrology, Phys. Dark Universe **26**, 100345 (2019).
[25] Catriona Thomson, Maxim Goryachev, Ben T. McAllister, and Michael E. Tobar, Corrigendum to "axion detection with precision frequency metrology", Phys. Dark Universe **26**, 100345 (2019); **32**, 100787 (2021).
[26] Catriona A. Thomson, Ben T. McAllister, Maxim Goryachev, Eugene N. Ivanov, and Michael E. Tobar, Upconversion Loop Oscillator Axion Detection Experiment: A Precision Frequency Interferometric Axion Dark Matter Search with a Cylindrical Microwave Cavity, Phys. Rev. Lett. **126**, 081803 (2021); **127**, 019901(E) (2021).
[27] Catriona A. Thomson, Maxim Goryachev, Ben T. McAllister, Eugene N. Ivanov, Paul Altin, and Michael E. Tobar, Searching for low-mass axions using resonant upconversion, Phys. Rev. D **107**, 112003 (2023).
[28] Robert Lasenby, Microwave cavity searches for low-frequency axion dark matter, Phys. Rev. D **102**, 015008 (2020).
[29] Robert Lasenby, Parametrics of electromagnetic searches for axion dark matter, Phys. Rev. D **103**, 075007 (2021).
[30] Asher Berlin, Raffaele Tito D'Agnolo, Sebastian A. R. Ellis, Christopher Nantista, Jeffrey Neilson, Philip Schuster, Sami Tantawi, Natalia Toro, and Kevin Zhou, Axion dark matter detection by superconducting resonant frequency conversion, J. High Energy Phys. 07 (2020) 088.
[31] Asher Berlin, Raffaele Tito D'Agnolo, Sebastian A. R. Ellis, and Kevin Zhou, Heterodyne broadband detection of axion dark matter, Phys. Rev. D **104**, L111701 (2021).
[32] J. F. Bourhill, E. C. I. Paterson, M. Goryachev, and M. E. Tobar, Twisted anyon cavity resonators with bulk modes of chiral symmetry and sensitivity to ultra-light axion dark matter, arXiv:2208.01640.
[33] Ben T. McAllister, Maxim Goryachev, Jeremy Bourhill, Eugene N. Ivanov, and Michael E. Tobar, Broadband axion dark matter haloscopes via electric field sensing, arXiv:1803.07755.
[34] Junxi Duan, Yu Gao, Chang-Yin Ji, Sichun Sun, Yugui Yao, and Yun-Long Zhang, Resonant electric probe to axionic dark matter, Phys. Rev. D **107**, 015019 (2023).
[35] Georg Engelhardt, Amit Bhoonah, and W. Vincent Liu, Detecting axion dark matter with Rydberg atoms via induced electric dipole transitions, arXiv:2304.05863.
[36] Michael E. Tobar, Ben T. McAllister, and Maxim Goryachev, Poynting vector controversy in axion modified electrodynamics, Phys. Rev. D **105**, 045009 (2022); **106**, 109903(E) (2022).
[37] Michael E. Tobar, Catriona A. Thomson, Benjamin T. McAllister, Maxim Goryachev, Anton V. Sokolov, and Andreas Ringwald, Sensitivity of resonant axion haloscopes to quantum electromagnetodynamics, Ann. Phys. (Berlin) 2200594 (2023).
[38] Ben T. McAllister, Aaron Quiskamp, Ciaran A. J. O'Hare, Paul Altin, Eugene N. Ivanov, Maxim Goryachev, and Michael E. Tobar, Limits on dark photons, scalars, and axion-electromagnetodynamics with the ORGAN experiment, Ann. Phys. (Berlin) 2200622 (2023).

[39] Tong Li, Rui-Jia Zhang, and Chang-Jie Dai, Solutions to axion electromagnetodynamics and new search strategies of sub-μev axion, J. High Energy Phys. 03 (2023) 088.
[40] Willy Fischler and John Preskill, Dyon-axion dynamics, Phys. Lett. **125B**, 165 (1983).
[41] Note that the couplings g_{aMM} and g_{aEM} arise in the theories which feature heavy magnetic monopoles; in the theories with both electric and magnetic charges, the charged particles in the classical low energy approximation have to be treated as essentially point-like.
[42] Michael E. Tobar, Ben T. McAllister, and Maxim Goryachev, Modified axion electrodynamics as impressed electromagnetic sources through oscillating background polarization and magnetization, Phys. Dark Universe **26**, 100339 (2019).
[43] Paul Kinsler, Alberto Favaro, and Martin W. McCall, Four Poynting theorems, Eur. J. Phys. **30**, 983 (2009).
[44] V. V. Flambaum, B. T. McAllister, I. B. Samsonov, and M. E. Tobar, Searching for scalar field dark matter using cavity resonators and capacitors, Phys. Rev. D **106**, 055037 (2022).
[45] Robert Leighton Feynman and Mathew Sands, *The Feynman Lectures on Physics: Chapter 23*, New Millennium edition (California Institute of Technology, New York, 2010), Vol. I.
[46] Michael E. Tobar, Catriona A. Thomson, William M. Campbell, Aaron Quiskamp, Jeremy F. Bourhill, Benjamin T. McAllister, Eugene N. Ivanov, and Maxim Goryachev, Comparing instrument spectral sensitivity of dissimilar electromagnetic haloscopes to axion dark matter and high frequency gravitational waves, Symmetry **14**, 2165 (2022).
[47] K. Saito, Breakdown phenomena in vacuum, in *Proceedings of the 1992 Linear Accelerator Conference*, edited by C. R. Hoffmann (JP Scientific (Nantwich) Ltd., UK, 1992), pp. 575–579.
[48] C. Hagmann, P. Sikivie, N. Sullivan, D. B. Tanner, and S.-I. Cho, Cavity design for a cosmic axion detector, Rev. Sci. Instrum. **61**, 1076 (1990).
[49] C. Hagmann, P. Sikivie, N. S. Sullivan, and D. B. Tanner, Results from a search for cosmic axions, Phys. Rev. D **42**, 1297 (1990).
[50] R. Bradley, J. Clarke, D. Kinion, L. J. Rosenberg, K. van Bibber, S. Matsuki, M. Muck, and P. Sikivie, Microwave cavity searches for dark-matter axions, Rev. Mod. Phys. **75**, 777 (2003).
[51] S. J. Asztalos, G. Carosi, C. Hagmann, D. Kinion, K. van Bibber, M. Hotz, L. J. Rosenberg, G. Rybka, J. Hoskins, J. Hwang, P. Sikivie, D. B. Tanner, R. Bradley, and J. Clarke, SQUID-Based Microwave Cavity Search for Dark-Matter Axions, Phys. Rev. Lett. **104**, 041301 (2010).
[52] J. Hoskins, J. Hwang, C. Martin, P. Sikivie, N. S. Sullivan, D. B. Tanner, M. Hotz, L. J. Rosenberg, G. Rybka, A. Wagner, S. J. Asztalos, G. Carosi, C. Hagmann, D. Kinion, K. van Bibber, R. Bradley, and J. Clarke, Search for nonvirialized axionic dark matter, Phys. Rev. D **84**, 121302 (2011).
[53] T. Braine *et al.*, Extended Search for the Invisible Axion with the Axion Dark Matter Experiment, Phys. Rev. Lett. **124**, 101303 (2020).
[54] C. Bartram *et al.*, Axion dark matter experiment: Run 1b analysis details, Phys. Rev. D **103**, 032002 (2021).
[55] Ben T. McAllister, Graeme Flower, Eugene N. Ivanov, Maxim Goryachev, Jeremy Bourhill, and Michael E. Tobar, The ORGAN experiment: An axion haloscope above 15 GHz, Phys. Dark Universe **18**, 67 (2017).
[56] Aaron Quiskamp, Ben T. McAllister, Paul Altin, Eugene N. Ivanov, Maxim Goryachev, and Michael E. Tobar, Direct search for dark matter axions excluding ALP cogenesis in the 63- to 67- micro eV range with the ORGAN experiment, Sci. Adv. **8**, eabq3765 (2022).
[57] Claudio Gatti, Paola Gianotti, Carlo Ligi, Mauro Raggi, and Paolo Valente, Dark matter searches at LNF, Universe **7**, 236 (2021).
[58] Y. Kishimoto, Y. Suzuki, I. Ogawa, Y. Mori, and M. Yamashita, Development of a cavity with photonic crystal structure for axion searches, Prog. Theor. Exp. Phys. **2021**, 063H01 (2021).
[59] Jack A. Devlin, Matthias J. Borchert, Stefan Erlewein, Markus Fleck, James A. Harrington, Barbara Latacz, Jan Warncke, Elise Wursten, Matthew A. Bohman, Andreas H. Mooser, Christian Smorra, Markus Wiesinger, Christian Will, Klaus Blaum, Yasuyuki Matsuda, Christian Ospelkaus, Wolfgang Quint, Jochen Walz, Yasunori Yamazaki, and Stefan Ulmer, Constraints on the Coupling between Axion-like Dark Matter and Photons Using an Antiproton Superconducting Tuned Detection Circuit in a Cryogenic Penning Trap, Phys. Rev. Lett. **126**, 041301 (2021).
[60] Ohjoon Kwon *et al.*, First Results from an Axion Haloscope at CAPP around 10.7 μeV, Phys. Rev. Lett. **126**, 191802 (2021).
[61] K. M. Backes, D. A. Palken, S. Al Kenany, B. M. Brubaker, S. B. Cahn, A. Droster, Gene C. Hilton, Sumita Ghosh, H. Jackson, S. K. Lamoreaux, A. F. Leder, K. W. Lehnert, S. M. Lewis, M. Malnou, R. H. Maruyama, N. M. Rapidis, M. Simanovskaia, Sukhman Singh, D. H. Speller, I. Urdinaran, Leila R. Vale, E. C. van Assendelft, K. van Bibber, and H. Wang, A quantum enhanced search for dark matter axions, Nature (London) **590**, 238 (2021).
[62] Aiichi Iwazaki, Axion-radiation conversion by super and normal conductors, Nucl. Phys. **B963**, 115298 (2021).
[63] So Chigusa, Takeo Moroi, and Kazunori Nakayama, Axion/hidden-photon dark matter conversion into condensed matter axion, J. High Energy Phys. 08 (2021) 074.
[64] Xunyu Liang, Egor Peshkov, Ludovic Van Waerbeke, and Ariel Zhitnitsky, Proposed network to detect axion quark nugget dark matter, Phys. Rev. D **103**, 096001 (2021).
[65] A. Álvarez Melcón *et al.*, First results of the CAST-RADES haloscope search for axions at 34.67 micro eV, J. High Energy Phys. 10 (2021) 075.
[66] D. Alesini, D. Babusci, C. Braggio, G. Carugno, N. Crescini, D. D'Agostino, A. D'Elia, D. Di Gioacchino, R. Di Vora, P. Falferi, U. Gambardella, C. Gatti, G. Iannone, C. Ligi, A. Lombardi, G. Maccarrone, A. Ortolan, R. Pengo, A. Rettaroli, G. Ruoso, L. Taffarello, and S. Tocci, Search for Galactic axions with a high-Q dielectric cavity, Phys. Rev. D **106**, 052007 (2022).
[67] CAST Collaboration, New CAST limit on the axion-photon interaction, Nat. Phys. **13**, 584 (2017).
[68] Ciaran O'Hare, cajohare/axionlimits: Axionlimits, https://cajohare.github.io/AxionLimits/ (2020).